

# Structural and magnetic properties of $\text{Fe}_x\text{O}_y$ nanoparticles dispersed in silica matrix

D. PREDOI<sup>\*</sup>, R. CLERAC<sup>a</sup>, M. RAILEANU<sup>b</sup>, M. CRISAN<sup>b</sup>, M. ZAHARESCU<sup>b</sup>

National Institute for Physics of Materials, P.O. Box. MG 07, 77125, Bucharest Magurele, Romania

<sup>a</sup>Centre de Recherche Paul Pascal, CNRS-UPR 8641, 115 avenue du Dr. A. Schweitzer, 33600 Pessac, France

<sup>b</sup>Institute of Physical Chemistry, "Ilie Murgulescu" Roumanian Academy, 202 Splaiul Independentei, 060021, Bucharest, Roumania

Some  $\text{Fe}_x\text{O}_y\text{-SiO}_2$  composites were prepared by the colloidal and alkoxidic route of the sol-gel method. The dried gels were thermally treated and the samples were characterized by X-ray diffraction (XRD), transmission electron microscopy (TEM), infrared absorption (IR) spectroscopy, magnetic susceptibility measurements and Mössbauer spectroscopy. Nanoparticles of  $\gamma$  and/or  $\alpha$  iron oxide phase of different size were obtained in the silica matrix depending on the gelation conditions and on the thermal treatment. It was observed that the particle sizes and the thermal stability of the iron oxide phases strongly depend on the preparation method. At temperatures above 400 °C, the  $\gamma$ -phase begins to transform to the  $\alpha$ -phase.

(Received November 12, 2007; accepted April 5, 2007)

**Keywords:** Nanocomposites,  $\text{Fe}_x\text{O}_y$  nanoparticles, Silica matrix

## 1. Introduction

The synthesis of materials in the nanometer range is of great interest due to their distinct optical, magnetic and chemical properties. The iron and iron-oxide based nanomaterials have potential applications in reading and writing technologies on magnetic media [1], in catalysis [2], color imaging [3], ferrofluids [4]. The preparation of nanocomposites by including the nanoparticles in a silica sol-gel matrix represents an effective remedy to the tendency of nanopowders to aggregate [5-10]. The use of an inorganic matrix as a host for nanocrystalline particles can provide an effective way for obtaining a particle-size distribution as well as for controlling the homogeneous dispersion of ultra-fine metal oxide particles. The physical properties of an assembly of magnetically ordered single domain nanoparticles dispersed in a diamagnetic matrix depend on a number of parameters which characterize the magnetic compound and the morphology of the nanoparticles.

In the present work, nanocomposite materials in the  $\text{Fe}_x\text{O}_y\text{-SiO}_2$  system were prepared by sol-gel method via alkoxide and aqueous route starting with a  $\text{Fe}^{3+}$  precursor, in order to accomplish a comparative study on their preparation conditions, structure and properties. The amorphous and crystalline state of the products and the size of the particles were controlled by X-ray diffraction (XRD) and transmission electron microscopy (TEM). The local order around  $\text{Fe(III)}$  ions was investigated by

Mössbauer spectroscopy. The magnetic properties were monitored by magnetic susceptibility measurements.

## 2. Experimental

### Preparation of samples

All the samples were prepared by the sol-gel method using two different routes: the alkoxidic and the aqueous one. The chemical composition and the experimental conditions for nanocomposites preparations are presented in Table 1. As iron source, the iron (III) nitrate nonahydrate [ $\text{Fe}(\text{NO}_3)_3 \cdot 9\text{H}_2\text{O}$ ] from Chimopar was used in both cases and its content in the nanocomposite material was calculated to be 10 wt.% related to the  $\text{SiO}_2$  content, respectively a molar ratio  $\text{Fe}/\text{SiO}_2$  equal to 1/8.37. The iron salt was introduced in the system as aqueous solution in all experiments. Concerning the silica precursor, a colloidal silica-sol Ludox AS-30, 30 wt% (Aldrich) was used for the aqueous route and tetraethoxysilane (TEOS) from Merck in the alkoxidic case. In the alkoxidic route, absolute ethanol (Riedel de Haen) as solvent and deionized water for hydrolysis has also been used. The syntheses were carried out on magnetic stirrers with controlled temperature in the reaction conditions presented in the table. The wet gels were dried at 80 °C for 24 h. According to the DTA/TGA results, the obtained gels were thermally treated for four hours at 350 °C using a heating rate of 1 °C/min [11].

Table 1. The chemical composition and the preparative conditions of the  $\text{Fe}_x\text{O}_y/\text{SiO}_2$  nanocomposites.

Sample	Sol-gel method route	Chemical composition			Reaction conditions		Gelation time (h)
		$\text{SiO}_2$		$\text{Fe}_2\text{O}_3^x$	pH	T(C)	
		Precursor <sup>xx</sup>	Molar ratio (MR)	$\text{Fe}/\text{SiO}_2(\text{MR})$			
S	Colloidal	SC	$\text{SiO}_2/\text{H}_2\text{O}=1/11.47$	1/8.37	2	65	2.5
T	Alkoxidic	TEOS	$\text{SiO}_2/\text{H}_2\text{O}/\text{C}_2\text{H}_5\text{H}=1/11.47/8$	1/8.37	2	65	2.25

<sup>x</sup> The source of  $\text{Fe}_x\text{O}_y$  was  $\text{Fe}(\text{NO}_3)_3 \cdot 9\text{H}_2\text{O}$ ;

<sup>xx</sup> SC – colloidal silica; TEOS – tetraethoxysilan

### Characterizations of samples

Structural evolution of the samples was monitored by XRD using  $\theta$ - $2\theta$  conventional equipment (Philips type PW1050) with  $\text{CuK}\alpha$  wavelength. In order to analyze the degree of dispersion of the particles in the matrix and the surface morphology of the samples transmission electron microscopy (TEM) measurements have been performed using a JEOL 200 CX equipment and using 100000 magnifications. For the TEM measurements the samples were milled and the obtained powders were dispersed in chemically pure acetone and dropped on conventional carbon coated copper grids.

The IR absorption spectra were performed in the 2000 to  $400\text{ cm}^{-1}$  range using a BX FT-IR spectrophotometer. The measurements were carried on powdered samples embedded in KBr pellets.

The Mössbauer absorption spectra were performed in a standard transmission geometry, using a  $^{57}\text{Co}$  source in rhodium (37 MBq). Calibration was performed using a 25  $\mu\text{m}$  thick natural iron foil: the isomer shift values are referred to  $\alpha$ -Fe. The measurements were carried out at room temperature on powdered samples using a Plexiglas sample holder. The surface density of the absorbers ranges from 105 to  $145\text{ mg/cm}^2$ .

The magnetic susceptibility measurements were performed on finely ground crystalline samples using a Quantum Design SQUID magnetometer MPMS-XL in the 1.8 to 400 K range and for dc applied fields ranging from -7 to 7 T. The magnetic data were corrected for the sample holder.

### 3. Results and discussion

In the Fig. 1 the XRD spectra of samples (T and S) heated at  $350\text{ }^\circ\text{C}$  for 2h are presented. In the case of sample S, the  $\alpha\text{-Fe}_2\text{O}_3$  phase is present. In sample T, an amorphous character of the silica matrix with a slight tendency to crystallize the  $\gamma\text{-Fe}_2\text{O}_3$  phase can be noticed. In the literature, the transition from  $\gamma$  to  $\alpha$  phase has been reported to occur at  $380\text{ }^\circ\text{C}$  for particles with an average size of 30 nm [12], and at  $500\text{ }^\circ\text{C}$  for particles of 10 nm [13]. It has also been observed that particles smaller than 10 nm in a  $\text{SiO}_2$  matrix continues to remain in  $\gamma$  phase up to  $1000\text{ }^\circ\text{C}$  [14]. For the prepared samples the average sizes calculated from the XRD peak broadening ( $D_{\text{RX}}$ ) were 12 and 5 nm, respectively. This indicates that the presence of  $\alpha$  phase in sample S is essentially due to the presence of larger particles which can easily be transformed to  $\alpha$  phase at  $400^\circ\text{C}$  [15]. The literature reports temperatures below  $400^\circ\text{C}$  for the transition from  $\gamma\text{-Fe}_2\text{O}_3$  to  $\alpha\text{-Fe}_2\text{O}_3$  phase in air atmosphere [16]. This limit of temperature can be raised by avoiding the particle aggregation. In fact, now it is well established that the transformation temperature is associated with the crystalline grain size [17-21].

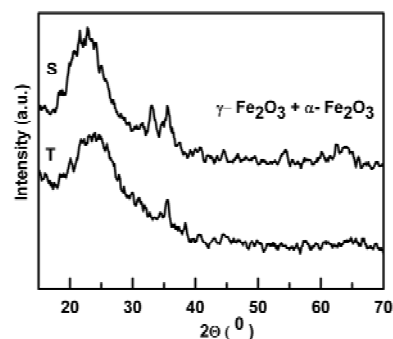


Fig. 1. The X-Ray diffraction pattern of S and T samples.

The particle size, their distribution and the degree of distribution of the particles in the matrix were visualized by TEM (Figs. 2 and 3). In TEM images, particles embedded into the  $\text{SiO}_2$  matrix are visible in both samples. In the S sample particles of approximately 15 nm size and in T sample particles of about 5 nm size have been observed.

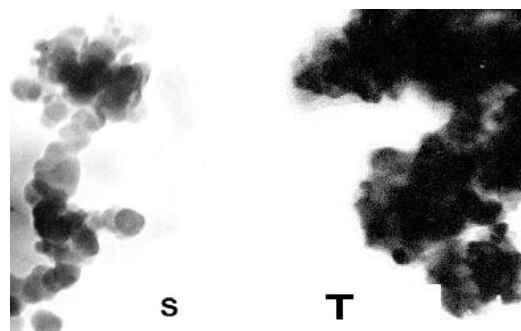


Fig. 2. TEM images of the S (left side) and T (right side) samples.

In the case of S sample, the presence of silica matrix together with an incipient crystallization of the iron oxide can be noticed. For the T sample, an increased degree of aggregation of silica compared with sample S can be observed. In this case, the iron oxide is embedded in the amorphous matrix, in agreement with the XRD results. It should be noted that for the prepared samples the size distributions of nanoparticles appears homogeneous dispersed in the silica matrix. The particles appear spherical in shape with average sizes smaller than 20 nm. TEM observations of the T sample show the presence of oxide particles. The dark-field micrograph indicates the amorphous character of a great number of nanoparticles.

In the FT-IR spectra of the prepared samples shown in the Fig. 3 the  $1640\text{ cm}^{-1}$  band is due to the bending of the adsorbed  $\text{H}_2\text{O}$  molecules which can interact through hydrogen bonds with silanol groups. We notice a lower intensity for the S sample. In all cases the characteristic vibration bands of a  $\text{SiO}_2$  gel were identified:  $\nu_{\text{as}}(\text{Si-O-Si})$  at  $1200\text{ cm}^{-1}$  and  $1075\text{ cm}^{-1}$ ;  $\nu_{\text{as}}(\text{Si-OH})$  at  $970\text{ cm}^{-1}$ ;  $\nu_{\text{s}}(\text{Si-}$

O-Si) at  $795\text{ cm}^{-1}$ ;  $\nu(\text{Si-O-Si})$  from cyclic tetramers at  $540\text{ cm}^{-1}$  and  $\delta(\text{Si-O-Si})$  at  $460\text{ cm}^{-1}$  in agreement with data from literature [5]. The band at  $950\text{ cm}^{-1}$  disappears for sample S indicating the polycondensation process [22-23]. The  $\nu(\text{Fe-O})$  vibration band ( $530\text{ cm}^{-1}$ ) appears distinctly only for sample T. For the S sample it is hidden by the overlapping with the vibration band characteristic to the silica matrix ( $540\text{ cm}^{-1}$ , Si-O-Si from cyclic tetramers).

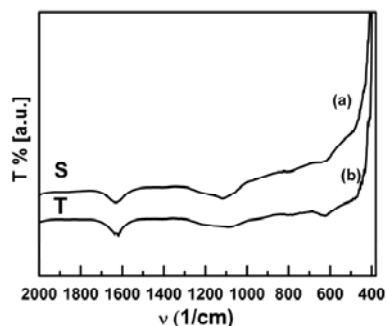


Fig. 3. FTIR spectra of S (curve a) and T (curve b) samples.

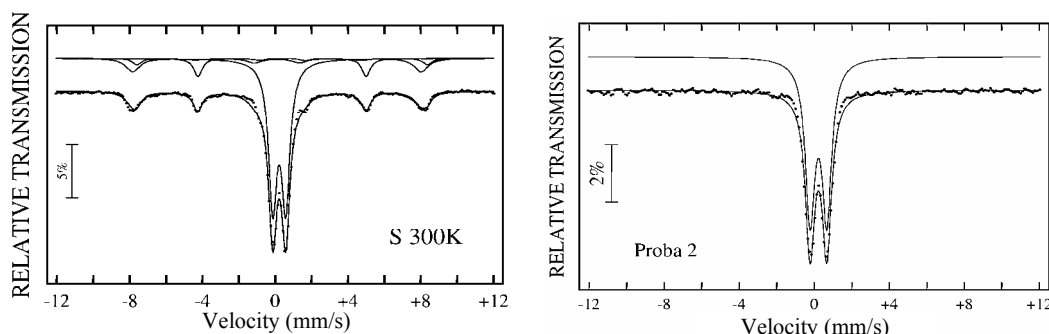


Fig. 4. Transmission Mössbauer spectra recorded at 300 K for S (left) and T (right) samples.

The magnetization ( $M$ ) vs magnetic field ( $H$ ) data at 100 K have been obtained with the use of a SQUID magnetometer (Fig. 5). The presence of a ferromagnetic phase is detected when a rapid increase of the magnetization is observed at low field, while a

The Mössbauer absorption spectra of the sample S is shown in Fig. 4a, while Fig. 4b shows the spectrum of sample T. The sample S is magnetically ordered while the T sample is in a paramagnetic state. At room temperature, the spectra of T sample (Fig. 4b) consist of a central doublet with an isomer shift of around  $0.28\text{ mm/s}$  according to a superparamagnetic behavior of the particles. All the spectra show components with values of IS typical of trivalent iron [24, 25].

The spectrum of sample S was fitted by two magnetic sextuplets and one doublet (Fig. 4a). The paramagnetic compounds are attributed to a superparamagnetic behavior. The sextuplets indicate the presence of magnetic order in the sample. The two components have magnetic fields smaller than those of the corresponding bulk phases, because of the nanocrystalline character of the particles [26]. Therefore it is impossible to assign the single components to precise phase. The second and third components can be attributed to maghemite in a mixture with hematite [27].

paramagnetic system will linearly respond. Therefore these data are in very good agreement with the Mössbauer data that shows a paramagnetic behavior for T while a ferromagnetic contribution is observed for S.

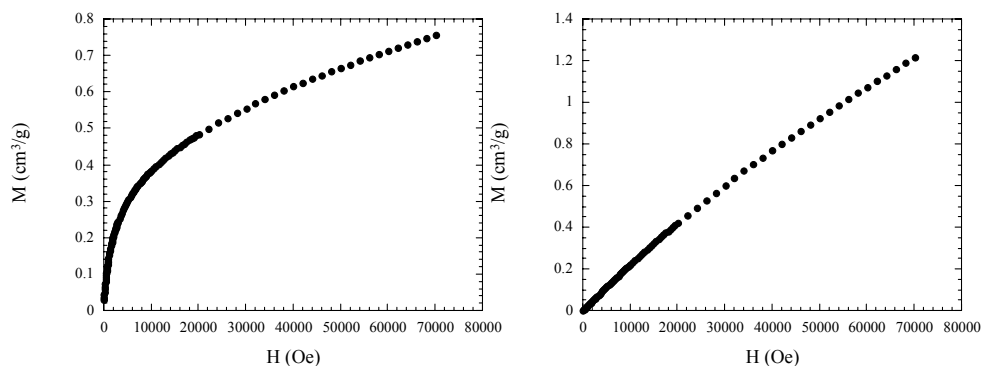


Fig. 5. The dependence of the magnetization ( $M$ ) on the applied field ( $H$ ) recorded at 100 K for the S (left side) and T (right side) samples.

#### 4. Conclusions

Some  $\text{Fe}_x\text{O}_y - \text{SiO}_2$  nanocomposites, in which the iron is present exclusively as Fe (III), were successfully prepared by the sol-gel method via aqueous and colloidal routes. All the experimental observations indicate that the nature of the particles changes during the thermal treatment which suggests that iron oxide particles are not present in a unique form. Using the colloidal route (sample S) the  $\gamma\text{-Fe}_2\text{O}_3$  and  $\alpha\text{-Fe}_2\text{O}_3$  phase have been detected. In the alkoxidic route (sample T) small particles with a paramagnetic behavior have been obtained. The differences between the two obtained  $\text{Fe}_x\text{O}_y - \text{SiO}_2$  nanocomposites are due to the type of host matrix resulted from the two routes of sol-gel synthesis used.

#### References

- [1] S. Onodera, H. Kondo, T. Kawana, *MRS Bull.* **21**, 35 (1996).
- [2] R. F. Ziolo, E. P. Giannelis, B. A. Weinstein, M. P. O'Horo, B. N. Ganguly, V. Metrotra, M. W. Russel, D. R. Huffman, *Science*, **257**, 219 (1992).
- [3] C. R. F. Lund, J. A. Dumesic, *J. Phys. Chem.* **86**, 130 (1982).
- [4] S. W. Charles, in *Studies of magnetic properties of fine particles and their relevance to materials science*, ed. J. L. Dormann and D. Fiorani. Elsevier Science, Amsterdam, 1992, p. 267.
- [5] S. Bruni, F. Cariati, M. Casu, A. Lai, A. Musinu, G. Piccaluga, S. Solinas, *NanoStructured Materials* **11**(5), 573-586 (1999).
- [6] G. Garçon, P. Gosset, F. Zerimech, B. Grave-Descampiaux, P. Shirali, *Toxicology Letters* **150**, 179-189 (2004).
- [7] K. Woo, H. J. Lee, *J. M. M. M.* **272-276**, e1155-e1156 (2004).
- [8] R. D. Shull, J. J. Ritter, A. J. Shapiro, L. J. Swartzendruber, L. H. Benet, *J. Appl. Phys.* **67**, 4490 (1990).
- [9] S. Roy, A. Chatterjee, D. Chakravorty, *J. Mater. Res.* **8**, 689 (1993).
- [10] P. J. Wang, H. L. Luo, *J. Appl. Phys.* **75**, 7425 (1994).
- [11] M. Raileanu, M. Crisan, C. Petrache, D. Crisan, M. Zaharescu, D. Predoi, *Revista Romana de Materiale*, vol. XXXIV, nr. 3, 189-195 (2004).
- [12] C. Chaneac, E. Tronc, J. P. Jolivet, *Nanostruct. Mater.* **6**, 715 (1995).
- [13] J. L. Dormann, D. Fiorani, E. Tronc, *Adv. Chem. Phys.* **283**, 98 (1997).
- [14] G. Ennas, A. Musinu, G. Piccaluga, D. Zedda, D. Gatteschi, C. Sangregorio, *J. Phys. Chem.* **10**, 495 (1998).
- [15] S. Solinas, C. Piccaluga, M. P. Morales, C. J. Serna, *Acta Mater.* **49**, 2805 (2001).
- [16] E. Herrero, M. V. Cabanas, M. Vallet-Regi, J. L. Martinez, J. M. Gonzalez-Calbet, *Solid State Ionics*, 101-103, 213 (1997).
- [17] P. Ayyub, M. Multani, M. Barma, V. R. Palkar, R. Vijayaraghavan: *J. Phys. C: Solid State Phys.* **21**, 2229 (1988).
- [18] N. Randrianantoandro, P. Laffez, C. Sella, J. M. Grenèche: *Eur. Phys. J.: Appl. Phys.* **9**, 125 (2000).
- [19] N. Randrianantoandro, A. M. Mercier, M. Hervieu, J. M. Grenèche, *Mater. Lett* **47**, 150 (2001).
- [20] F. Mathieu, P. Roux, G. Bonel, A. Rousset, C. R. Acad. Sci. Paris Ser. **305**, 249 (1987).
- [21] E. Tronc, C. Chaneac, J. P. Jolivet, *Proc. Fifth Int. Workshop Non-Cryst. Solids*, ed. By J. Rivas, M.A. Lopez-Quintela (World Scientific, Singapore 1997), p. 262.
- [22] C. Chaneac, E. Tronc, J. P. Jolivet, *J. Mater. Chem.* **6**(12), 1905 (1996).
- [23] C. A. Capozzi, L. D. Pye, R. A. Condrate – Vibrational spectral/structural changes from the hidrolisis/polycondensation of methyl – modified silicates. Comparisons for single monomer condensates – *Mat. Lett.* **15**, 130 (1992).
- [24] P. Gutlich, R. Link, A. Trautwein, "Mossbauer Spectroscopy and Transition Metal Chemistry; Springer-Verlag: Berlin, 1978; p. 56.
- [25] M. Darby Dyar, *Am. Mineral.* **70**, 304 (1985).
- [26] S. Morup, H. Topsoe, J. Lipka, *J. Phys.* **35**, C6-207 (1976).
- [27] R. Zboril, M. Mashlan, D. Petridis, *Chem. Mater.* **14**, 969 (2002).